Mechanical stochastic tug-of-war models cannot explain bidirectional lipid-droplet transport

Ambarish Kunwar[a,1], Suvranta K. Tripathy[b,1], Jing Xu[b,c], Michelle K. Mattson[b], Preetha Anand[b], Roby Sigua[b], Michael Vershinin[d], Richard J. McKenney[e], Clare C. Yu[f], Alexander Mogilner[a,2,3], and Steven P. Gross[b,2,3]

[a]Department of Neurobiology, Physiology and Behavior, University of California, Davis, CA 95616; [b]Department of Developmental and Cell Biology, University of California, Irvine, CA 92697; [f]Department of Physics and Astronomy, University of California, Irvine, CA 92697; [d]Department of Physics and Astronomy, University of Utah, Salt Lake City, UT 84112; and [e]Department of Pathology and Cell Biology, Columbia University, New York, NY 10032 [c]School of Natural Sciences, University of California, Merced, CA 95343

Edited by Charles S. Peskin, New York University, New York, NY, and approved September 15, 2011 (received for review May 18, 2011)

Intracellular transport via the microtubule motors kinesin and dynein plays an important role in maintaining cell structure and function. Often, multiple kinesin or dynein motors move the same cargo. Their collective function depends critically on the single motors' detachment kinetics under load, which we experimentally measure here. This experimental constraint—combined with other experimentally determined parameters—is then incorporated into theoretical stochastic and mean-field models. Comparison of modeling results and in vitro data shows good agreement for the stochastic, but not mean-field, model. Many cargos in vivo move bidirectionally, frequently reversing course. Because both kinesin and dynein are present on the cargos, one popular hypothesis explaining the frequent reversals is that the opposite-polarity motors engage in unregulated stochastic tugs-of-war. Then, the cargos' motion can be explained entirely by the outcome of these opposite-motor competitions. Here, we use fully calibrated stochastic and mean-field models to test the tug-of-war hypothesis. Neither model agrees well with our in vivo data, suggesting that, in addition to inevitable tugs-of-war between opposite motors, there is an additional level of regulation not included in the models.

Bidirectional motion of subcellular cargos such as mRNA particles, virus particles, endosomes, and lipid droplets is quite common (1), driven by plus-end kinesin and minus-end dynein. Bidirectional motion emerges when frequent switches occur between travel directions, and travel direction reflects which motor (s) dominates. Cells can regulate the switching frequency to control "net" transport, but the physical mechanism(s) underlying this control remains open. Two mechanisms have been proposed. The first suggests that plus-end and minus-end motors always engage in stochastic unregulated tugs-of-war, and overall cargo motion is explained by the outcomes of these mechanical tugs-of-war. This model was proposed theoretically to explain lipid-droplet motion (2) but has been adopted to explain endosome motion (3, 4). An alternative model suggests that in addition to competition between opposite-polarity motors, there is a "switch" mechanism or mechanisms that achieve further coordination between the motors. Such regulation may be dynamic (5), static (6), or a combination of the two. The crucial question is this: Can tug-of-war models, which exclusively consider cargos with fixed distributions of motors moving along microtubules unaffected by regulatory pathways, explain the characteristics of motility in vivo? Alternatively, are there significant motility characteristics not captured by tug-of-war models, pointing to a richer transport subsystem with important regulatory contributions?

There are two theoretical approaches to modeling collective motor transport. The mean-field approach (Fig. 1*A*) assumes all engaged motors share load equally (7). The stochastic model (Fig. 1*B*) simulates individual motors going through their mechanochemical cycle (8), where each motor's movement is determined by the load the cargo applies to that motor. The external load on the cargo and instantaneous positions of each motor define the cargo's position. Thus, different motors in the group move with different rates and experience different instantaneous forces; the cargo mechanically couples the motors. Each unidirectional model is the basis for a corresponding bidirectional tug-of-war model (Fig. 1 *C* and *D*).

Here, we consider both classes of models and compare theoretical predictions with experimentally observed motility. We start with models maximally constrained by experimental observations of single-motor behavior and then relax these constraints to investigate both quantitative and qualitative differences between model predictions and actual data. We note that motor detachment kinetics under high load affect motors' ensemble function (9), but complete data was not available. We thus measured single-motor detachment kinetics in the superstall regime and used this to constrain the models. The stochastic unidirectional model quantitatively captured multiple-motor function as measured experimentally in vitro, but the mean-field model did not. In vivo, neither model explains bidirectional lipid-droplet motion.

Results

Experimental Measurement of Kinesin and Dynein Detachment Kinetics. Kinesin's superforce off rate was reported as 2/s (10), and limited measurements showed that dynein's off rate slightly above stall was about 10/s (9). Here, we measured the off rates more systematically, using an optical trap–based method. We rapidly increased the force on a moving bead (*SI Text*) and measured the time to detachment (Fig. 2*A*, kinesin; Fig. 2*B*, dynein). From such events, we determined the detachment time distributions for specific superforce values, shown, e.g., for kinesin and dynein at approximately twice the stall force (Fig. 2 *C* and *D*) (see also *SI Text*). The detachment times for each superforce value are summarized for kinesin (Fig. 2*E*) and dynein (Fig. 2*F*). In contrast to a possible constant off rate (10), kinesin had an off rate increasing with force. At low loads, dynein is sensitive to load, detaching easily (9), but at higher load it exhibited a catch-bond type behavior, with off rate decreasing with load. The superforce experiments also allowed us to determine the probability of backward stepping for the motors. Kinesin (11) and dynein (12) can back-step under load, but this was relatively rare in both directions (<20%), and the typical backward travel distance was short, so we believe it is functionally irrelevant with regard to the behavior of kinesin or

Author contributions: A.K., S.K.T., C.C.Y., A.M., and S.P.G. designed research; A.K. and S.K.T. performed research; A.K., S.K.T., J.X., M.K.M., P.A., R.S., M.V., and R.J.M. contributed new reagents/analytic tools; A.K., S.K.T., A.M., and S.P.G. analyzed data; and A.K., S.K.T., A.M., and S.P.G. wrote the paper.

The authors declare no conflict of interest.

This article is a PNAS Direct Submission.

[1]A.K. and S.K.T. contributed equally to this work.

[2]A.M. and S.P.G. contributed equally to this work.

[3]To whom correspondence may be addressed. E-mail: mogilner@math.ucdavis.edu or sgross@uci.edu.

This article contains supporting information online at www.pnas.org/lookup/suppl/doi:10.1073/pnas.1107841108/-/DCSupplemental.

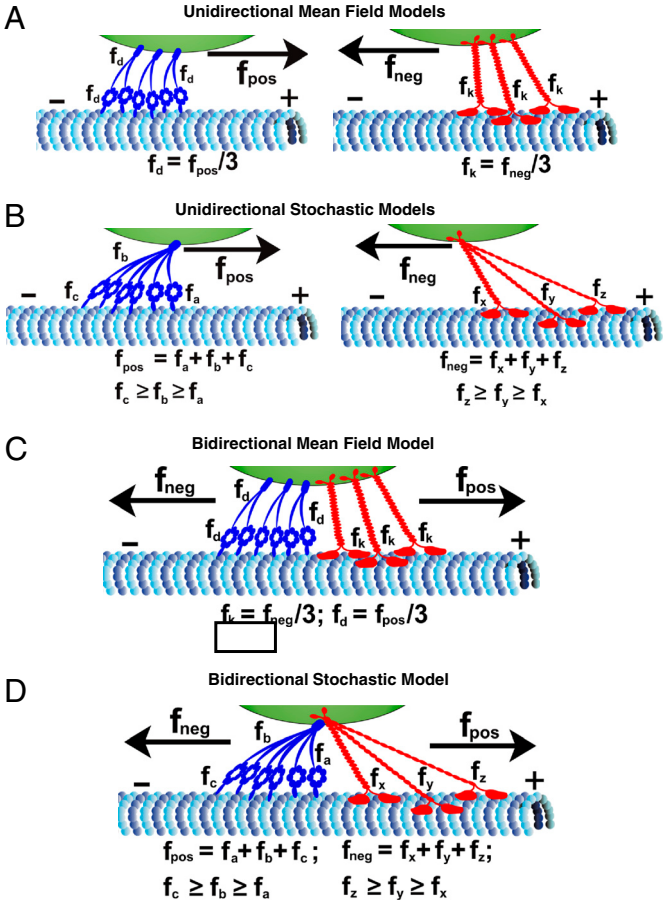

Fig. 1. Models of unidirectional (*A* and *B*) and bidirectional (*C* and *D*) transport schematic illustrations of a cargo (green) moved by $N = 3$ kinesin (red) or dynein (dark blue) motors, as modeled by the mean-field theory (*A*) or the stochastic model (*B*). Overall forces opposing motion (f_{pos},f_{neg}) are distributed equally in the mean-field model (f_d per dynein, f_k per kinesin), but not in the stochastic model (f_a–f_c for dynein, f_x–f_z for kinesin). (*C* and *D*) A tug-of-war between kinesin and dynein, as modeled in the mean-field theory (*C*) where motors share load equally, or the stochastic model (*D*) where they need not.

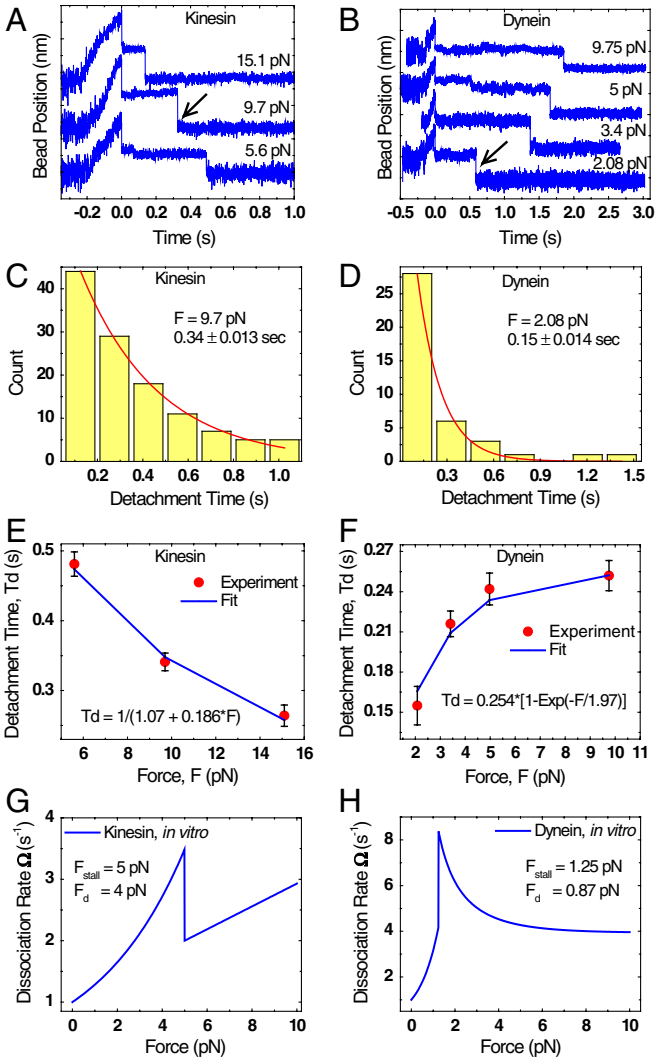

Fig. 2. Experimental characterization of in vitro single-molecule kinesin and dynein detachment kinetics. (*A* and *B*): Examples of experimental data traces. Beads with a single active kinesin (*A*) or dynein (*B*) (binding fraction < 0.35) were brought in contact with the microtubule at saturating ATP. Motion started (at approximately −0.2 s in these plots), causing displacement of the bead from the optical-trap center (traces start increasing). At a predefined displacement (here occurring at $t = 0$), the laser power was automatically increased, applying enough force to stall the moving bead (plateau immediately after $t = 0$). After a delay, the motor detached from the microtubule (black arrow), allowing the bead to rapidly return to the trap center. By controlling optical-trap power, we controlled the applied force. The detachment time was the interval between when trap power increased and when the bead detached; a histogram of such times is shown for one specific force for kinesin (*C*) and dynein (*D*). The characteristic detachment times were determined by fitting with decaying exponentials (red curves in *C* and *D*); the results of such fits are summarized in *E* and *F* for kinesin and dynein, respectively. *G* and *H* show the complete in vitro force-dissociation rate curves including detachment probabilities below stall (see *SI Text*).

dynein ensembles opposing each other. It was not included in our theoretical model.

Development of a Stochastic Unidirectional Theoretical Model for Kinesin and Dynein. Our older stochastic models for kinesin (8), and dynein (9, 13) were experimentally verified under some conditions (8, 9, 13). Here, we incorporate the measured detachment data into these models. The force-dissociation rate below stall is given by $\Omega(F) = \exp(F/Fd)$, as determined previously to match experimental data (8, 9). In the superstall regime, it was obtained by using simple fitting functions to approximate the measured detachment rates in Fig. 2 *E* and *F*. For kinesin, it was $\Omega(F) = 1.07 + 0.186 * F$, and for dynein was $\Omega(F) = 1/(0.254 * [1 - \exp(-F/1.97))$. The stall forces for kinesin and dynein were 4.7 ± 0.04 pN and 1.36 ± 0.02 pN, respectively, determined from in vitro stall-force distributions (see the *Definitions of the Stall Force (F_s) and Detachment Force (F_d) and Their Measurements* section in *SI Text*). F_d was the average detachment force obtained from experimental data (4.01 ± 0.07 pN for kinesin and 0.87 ± 0.04 pN for dynein). The dissociation rate near stall may be smoother than assumed in our model, but the model correctly captures the decline of the dissociation rate above stall. Associated corrections, if any, are not expected to alter the conclusions of this paper. The complete force-dissociation relations in our model are summarized in Fig. 2 *G* and *H* (see also *SI Text*).

Comparison of Stochastic and Mean-Field Theories with in Vitro Experiments for Unidirectional Motion: Detachment Times for Two-Motor Superstall Experiments. We experimentally tested the newly constrained theories using detachment times under superstall for two-motor events. With moderate motor density, beads are mostly moved by single motors, but are occasionally moved by two (motor density is chosen to make three-motor events rare). If a bead in a parabolic potential produced by an optical trap moved past a well-defined threshold force (slightly larger than F_s for a single motor), it was moved by two motors, and software increased the laser power abruptly to put the two motors into the

superstall regime. We then measured the detachment time distribution, for either kinesin (Fig. 3*A*) or dynein (Fig. 3*B*).

Constrained experimentally by measured single-molecule properties, and setting the total number of motors N equal to 2 instead of 1, there is only a single "free" parameter for the models, the single-motor on rate. Others have measured this to be approximately 5/s for kinesin (at saturating microtubule concentration), so we used this value; for dynein, it was a fitting parameter, and 5/s yielded the best description of the data. From the experimental distributions we calculated the mean detachment time, and then compared this with the predicted mean detachment times for the stochastic and mean-field theories (Fig. 3 *A* and *B*). The stochastic theory's predictions were consistent with experiments, but the mean-field predictions were not (Fig. 3 *C* and *D*), either when we assumed real experimental detachment kinetics, or when we assumed nonexperimental exponential detachment kinetics as has been done previously (7). Relative to the mean-field model, motors in the stochastic model were less sensitive to detachment under load (see *SI Text*).

The in Vivo Case: Model for a Bidirectional Tug-of-War. Given the stochastic model's in vitro success, we used it to develop a bidirectional tug-of-war model. We used the in vitro–measured detachment kinetics above stall, and other experimental constraints. First, our previous in vivo measurements established that in the absence of specific mutations, the forces powering plus-end and minus-end lipid-droplet motion were approximately the same (14), so any theoretical model must conform to this. Second, although the mechanism is currently unknown, our in vivo data suggests that the unitary (single-motor) stall force in each direction is approximately 2.5 pN, which is different from its value in vitro, so we decreased the kinesin stall force, and increased the dynein stall force (resulting in scaled force-dissociation curves shown in *SI Text*). Third, our recent quantitative measurements of droplet motion in phase II of *Drosophila* development (14) indicated that typically a few, but up to a maximum of four to five, motors could be instantaneously active. We assumed that in vivo on rates are the same as in vitro (i.e., approximately 5/s for both kinesin, and dynein) and that the motors had the same stiffness in vivo as in vitro. To constrain processivity, we purified kinesin from *Drosophila* embryos, and measured its single-molecule processivity to be 1.3 μm (*SI Text*). We have not yet determined *Drosophila* dynein's processivity, but assume it to be the same as for bovine dynein in the presence of dynactin (approximately 2.0 μm). With these constraints, we developed a stochastic tug-of-war model, as indicated in Fig. 1*D*. We estimate that the effective cytosolic viscosity affecting droplet motion is approximately 10× that of water, so that value was used in the simulations.

Thus, we implemented a bidirectional stochastic model with $N = 5$ motors. After incorporating the above experimental constraints, there were no free parameters; the model yielded simulated traces such as those shown in Fig. 4*B*. Using our parsing program (15), these traces were processed in the same way as for real motion, and a variety of metrics were compared to experimental values (see next).

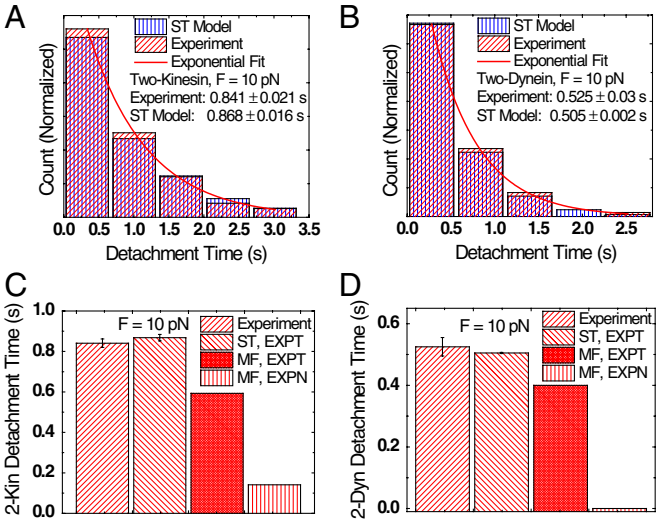

Fig. 3. Comparison of experimental measurements and theoretical predictions for detachment kinetics of two kinesin or dynein motors. Experiments were done as in Fig. 2 *A* and *B*, but a higher concentration of motors was used, so there was a small probability of having two simultaneously engaged motors. These relatively rare events were detected by force measurements: When a bead was moved further from the trap center than possible for a single motor (experimentally a threshold of 5.2 and 2.0 pN was used, for kinesin or dynein, respectively), the laser power was automatically increased to provide a superstall force. The distribution of detachment times (experimental bars, red hash marks; *A* and *B*) was compared to theory (parameter values in *SI Text*). The single-molecule properties (including single-motor detachment kinetics as measured in Fig. 2) constrained the model parameters. Using these constraints, the stochastic model (ST) with experimental detachment kinetics (EXPT) correctly predicted both the shape of the detachment distribution (*A* and *B*) and the correct average detachment time for both kinesin and dynein (*C* and *D*, respectively). The mean-field model with the same detachment kinetics did not, and the mean-field model with exponential detachment kinetics (EXPN) was even worse.

Comparing in Vivo Experimental Data to the Stochastic Bidirectional Model. Our past studies developed multiple metrics to charac-

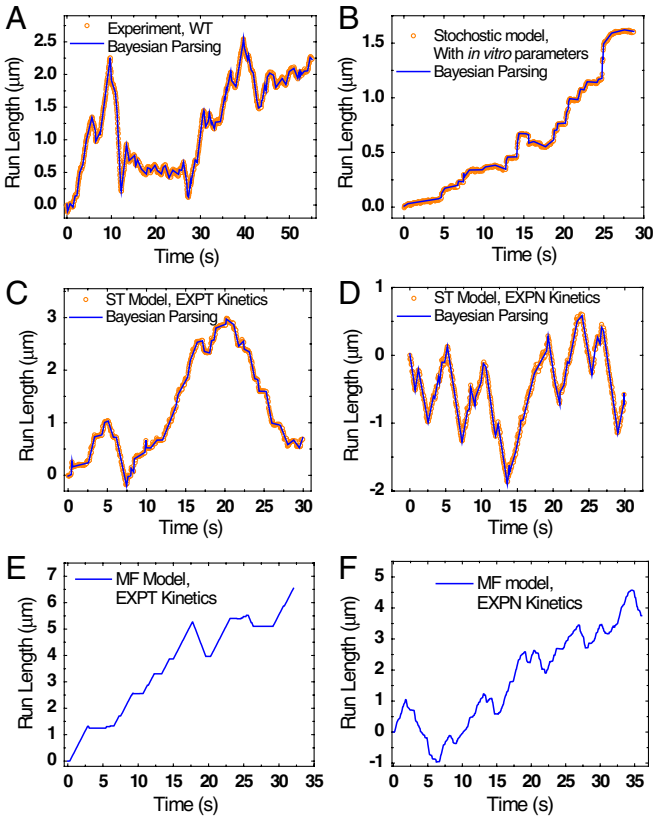

Fig. 4. Examples of experimental (*A*) and simulated (*B–F*) trajectories of single bidirectionally moving lipid droplets, projected along the axis of microtubules. For experimental data (*A*) and stochastically simulated motion (*B–D*), the properties of motion (run lengths and velocities, pause durations, etc.) were determined by parsing the motion identically using a Bayesian approach (15). The blue line corresponds to run and pause segments as parsed. For the mean-field model variants (*E* and *F*), the segments were determined directly.

terize motion. Individual lipid droplets are tracked using image processing combined with differential interference contrast microscopy, allowing us to determine the position of individual droplets with few-nanometer resolution at 30 frames per second. The trajectories of motion are projected along the microtubule axis, and then a Bayesian statistical approach (see ref. 15) is used to parse the motion into plus-end runs, minus-end runs, and pauses, taking into account the uncertainties in tracking and thermal noise effects (Fig. 4*A*). From this analysis, we extract velocities, lengths of plus-end and minus-end runs, and the frequency and duration of pauses.

With the stochastic model maximally constrained by experiments as discussed above, the predicted motion was quite different from what was observed experimentally: Runs (periods of uninterrupted motion) were very short (Fig. 4*B*), and approximately unidirectional, in contrast to the longer back-and-forth motion experimentally observed (Fig. 4*A*). Further, the predicted motion spent much more time paused than what was observed experimentally [Table 1, third (ST, 5 K ~ 5 D, NoTuning) row].

Because the completely constrained model failed, we considered variants by relaxing specific constraints. We started by adjusting the motors' on rates, which could be somewhat different from their in vitro values, because of the presence of proteins such as dynactin and the microtubule-associated proteins present in vivo but absent in vitro. The "untuned" case initially investigated exhibited excessive interruption from opposite motors, so we decreased on rates to decrease the frequency of potential tugs-of-war, until we matched the mean values of the wild-type run-length and velocity data reasonably well with the simulations [Table 1, fourth (ST, 5 K ~ 5 D, EXPT, WT) row]. However, the rate-adjusted model did not capture certain features. Experimentally [Table 1, first (Experiment, WT, N) row], in the wild type, droplets spend about 24% of the time paused, but in the stochastic simulation with $N = 5$ motors of each type, pauses were still too frequent, and motion was predicted to be paused 48% of the time. Because our experiments are quite reproducible, and the experimental variation is only a few percent, this theoretical prediction was considered to deviate significantly from reality. Furthermore, the stalls were too long, predicted to be about 0.68 ± 0.02 s vs. the experimentally observed pauses with a duration of 0.5 ± 0.003 s.

In addition to the incorrect pausing frequency and duration, the distribution of run lengths was not completely correct. Experimentally, the distribution of bidirectional runs is frequently described by the sum of two decaying exponentials (16), and our Bayesian analysis (15) previously determined that this is a real feature of the underlying motion and not an artifact due to thermal noise or other uncertainties. Indeed, our wild-type experimental data is described by such a distribution (*SI Text*), as were the simulated runs in the minus-end direction, but this was not true for the plus-end simulated data, which can be fit by a single decaying exponential (*SI Text*).

Given these discrepancies, we considered other possibilities. Stall durations were too long, so we decreased the total motor number, N, present on the droplets. This would be consistent with the observation that the pauses were too frequent [compare "time between pauses," in first (Experiment, WT, N) row to fourth (ST, 5 K ~ 5 D, EXPT, WT) row in Table 1), because we hypothesized that pauses occurred when there is a tug-of-war between opposite motors, and the larger the N, the larger the probability of such a tug-of-war occurring. Stall forces measured experimentally suggest that a maximum of $N = 5$ motors are engaged, but many times only a few motors were instantaneously active; perhaps most droplets are moved by fewer than five motors. We therefore considered a stochastic model with $N = 2.5$ motors, that is a mixed population where 50% of the droplets had $N = 3$ motors, and the others had $N = 2$ motors (a choice lower than $N = 2.5$ would be clearly inconsistent with experiments). We adjusted on rates and velocities to match wild-type observations. Results were somewhat better [Table 1, sixth (ST, 2.5 K ~ 2.5 D, EXPT, WT) row]: The percentage of time paused was 26%, consistent with the experimental value of 24%, and time between pauses was reasonable. Further, approximately 65% of the reversals in travel direction were rapid (with no obvious pause between), consistent with the experimental observation of 65%. The mean run lengths and velocities were also acceptable.

The stochastic model with $N = 2.5$ was thus considerably better than the $N = 5$ case, though there was still a discrepancy with the actual experimental data, in that the pause duration was now too short (Table 1). Interestingly, the distribution of plus-end run lengths was now appropriately modeled by a double-decaying exponential distribution (*SI Text*), though the contribution of the fast-decay component was small; the minus-end runs were still reasonably modeled by such a distribution (*SI Text*).

Table 1. Table of run length and pause behavior

Parameter characterized	% duration paused	Time between pauses, s	% of quick reversal, out of run segments	Pause duration, s	Positive run length, nm (skip pause)	Negative run length, nm (skip pause)
Experiment, WT, *N*	24%	3.57	65%	0.524 ± 0.003	558 ± 21	431 ± 21
Experiment, KHC, *N*/2	21%	3.89	63%	0.518 ± 0.004	695 ± 23	588 ± 24
ST, 5 K ~ 5 D, NoTuning	85%	1.78	16%	1.298 ± 0.024	365 ± 14	104 ± 3
ST, 5 K ~ 5 D, EXPT, WT	48%	2.03	45%	0.679 ± 0.020	550 ± 15	395 ± 15
ST, 2.5 K ~ 2.5 D, EXPT, Mut	29%	2.59	59%	0.478 ± 0.013	639 ± 27	486 ± 30
ST, 2.5 K ~ 2.5 D, EXPT, WT	26%	3.03	65%	0.445 ± 0.005	581 ± 19	473 ± 23
ST, 1.5 K ~ 1.5 D, EXPT, Mut	13%	4.74	77%	0.383 ± 0.009	585 ± 27	570 ± 40
ST, 5 K ~ 5 D, EXPN, WT	3%	15.68	95%	0.213 ± 0.006	584 ± 14	436 ± 15
ST, 2.5 K ~ 2.5 D, EXPN, Mut	2%	17.17	94%	0.185 ± 0.019	652 ± 25	494 ± 29
ST, 3 K ~ 12 D, EXPT, WT	38%	2.38	54%	0.502 ± 0.004	540 ± 15	417 ± 16
ST, 1.5 K ~ 6 D, EXPT, Mut	23%	3.01	65%	0.360 ± 0.005	599 ± 22	554 ± 35
MF, 5 K ~ 5 D, EXPT, WT	48%	1.6	5%	0.770 ± 0.009	530 ± 10	420 ± 19
MF, 2.5 K ~ 2.5 D, EXPT, Mut	56%	1.84	4%	1.043 ± 0.021	597 ± 21	478 ± 29
MF, 5 K ~ 5 D, EXPN, WT	10%	4.06	15%	0.403 ± 0.002	583 ± 5	452 ± 5
MF, 2.5 K ~ 2.5 D, EXPN, Mut	14%	2.84	19%	0.390 ± 0.004	367 ± 5	402 ± 6

The tug-of-war process involves competition between opposite motors and results in pauses in motion if this competition is not immediately resolved. The pause kinetics thus provides quantitation of tugs-of-war, so we focus on them both experimentally and theoretically. In several cases, two adjacent rows are related to each other. For instance, the experimental characterization of motion in the wild type is in the first row, and the experimental characterization of motion in the mutant background where there is half as much kinesin is in the second row. Similarly, the fourth row shows the prediction from the stochastic (ST) model for five kinesins (5 K) vs. five dyneins (5 D), with experimental detachment kinetics (EXPT), tuned to match the experimental data by adjusting the motors' on rates. Then, the fifth row is the prediction of the same model, with the same parameters and no tuning, with only the number of motors present changed to be $N = 2.5$ motors. The only unpaired row is row 3, which represents the stochastic model's prediction when completely constrained to use in vitro parameters. EXPN, exponential detachment kinetics.

Critical Test of the Stochastic Theory: Prediction of Motion in a Decreased Kinesin Heavy Chain (KHC) Background. Many aspects of this $N = 2.5$ version of the stochastic model [Table 1, sixth (ST, 2.5 K ~ 2.5 D, EXPT, WT) row] were acceptable, so we tested it further. A good way to test a theory is to fix unknown parameters by fitting experimental data under one in vivo condition, and then use the theory (with fixed parameters) to predict what should occur in a second in vivo condition where any changes in parameters are known/measured a priori [see, e.g., the prediction of lysosomal run lengths in neurons, as affected by decreasing dynein processivity (13)]. Here, we took such an approach. Using a kinesin-null mutation KHC-27 (which makes no protein), we created embryos from KHC-27/+ mothers, that is, mothers that had one null and one wild-type copy of the gene (14). In this background, lipid droplets are moved by 50% less kinesin (as determined by biochemistry, measuring droplet-bound kinesin, and by force measurements, assessing the number of active motors) (14). Thus, by construction, instead of $N = 2.5$, in this new background $N \approx 1.25$; for simplicity (and also to match experimental constraints, which clearly indicate significant contribution from a second motor in the mutant case), we modeled this theoretically using an equal combination of $N = 1$ and $N = 2$ droplets. Force measurements indicate that the number of active dynein motors was also decreased by 50% (14); such feedback is common, and has been observed in a number of systems (17), although its mechanistic underpinnings are unknown. We looked at the same developmental phase as for the wild-type embryos, so we used the same values of all the adjustable parameters that we fixed by fitting the wild-type motion. With these constraints, there are no adjustable parameters.

In this test, the stochastic $N = 1.5$ theory [Table 1, seventh (ST, 1.5 K ~ 1.5 D, EXPT, Mut) row] failed to correctly reproduce the experimental observations in a number of qualitative as well as quantitative ways. First, the stochastic model simulations predicted that the percentage of time paused decreased (from 26% to 13%). This was theoretically expected (given the pause frequency differences between the $N = 5$ and $N = 2.5$ simulations, and see discussion in *SI Text*), but not what was observed experimentally, where total time paused was approximately constant within experimental error [24% vs 21%; Table 1, first (Experiment, WT, N) row vs. second (Experiment, KHC, $N/2$) row]. Similarly, theoretically, the time between pauses increased dramatically [Table 1, seventh (ST, 1.5 K ~ 1.5 D, EXPT, Mut) row vs. sixth (ST, 2.5 K ~ 2.5 D, EXPT, WT) row], and pause duration decreased, because of fewer engaged motors, but this was not observed experimentally. Finally, experimentally, the decrease in N resulted in longer run lengths in both directions, but in theory, the effect was not observed in the plus-end direction, and the predicted increase in minus-end run length (21%) was smaller than observed (36%). Thus, although some of the model predictions were qualitatively in agreement with the experimental data (e.g., the predicted increase in velocities in each direction), some were not (pause frequencies and durations, and plus-end run lengths increasing), and even those that had a correct trend had magnitudes that were not consistent with experiments. We conclude that although the stochastic tug-of-war model with actual in vitro detachment kinetics and in vitro processivities recovers some of the features observed in the wild-type motion, it is not an accurate model of the experimental process.

Additional Variants. Overall, we considered relaxing a number of other constraints, including adjusting single-motor processivity, trying exponential instead of experimentally measured detachment kinetics, and allowing uneven numbers of motors (see *SI Text* for details). We also investigated mean-field tug-of-war models in addition to the stochastic models (see *SI Text*). None of these variants correctly described the data (see *SI Text* and Table 1).

Discussion

Experimental Measurements and Their Ramifications. Our recent NudE/Lis1 studies (9) highlight the importance of single-motor detachment kinetics for ensemble function under load; such kinetics are expected to be of particular importance in determining outcomes of hypothetical tugs-of-war between groups of motors. We systematically measured both kinesin and dynein detachment kinetics in vitro, and found neither as expected. Dynein had "catch-bond" detachment kinetics, with its detachment rate decreasing with increasing load. This could, in principle, contribute to dynein being able to serve as an "anchor" to hold subcellular organelles in place (18) under high load. We expect that these characterizations of the motors' detachment kinetics will be useful for theoretical models describing how ensembles of motors function together. We constrained two classes of models—stochastic and mean-field—by these data and compared their predictions to ensemble motor behavior in vitro. The stochastic model describes the in vitro data reasonably well, but the mean-field theory model does not.

Tug-of-War Scenarios to Explain Bidirectional Motion. Many cargos move bidirectionally, reversing travel direction every few seconds. The key determinant in net, or average transport, is the duration of runs (periods of travel between reversals) in each direction. Because run length is determined by reversal frequency, it is important to understand the reversal process. Tug-of-war models are appealing because they suggest that the reversals reflect unregulated (stochastic and mechanical) competitions between opposite-polarity motors on the cargo (a group of plus-end kinesins and a group of minus-end dyneins), allowing us, in principle, to use single-motor properties measured in vitro to predict and understand emergent transport in vivo.

We evaluated such models critically, within the context of lipid-droplet (LD) motion in *Drosophila* embryos, using a strategy previously used studying multiple dynein motors in vivo, in cultured neurons. We constrained the models' "free" parameters as much as possible via experimental data and then determined the values of any unconstrained parameters by fitting the theory's predictions to one experimental set of in vivo (wild-type) data. Once the theory's parameters were fixed, it was used to predict the outcome of a known change, with no further adjustment. In the previous study, modeling essentially unidirectional transport (13), the "known change" was a (in vitro measured) reduction in single-motor processivity, caused by the dynein Loa mutation. Here, the known change was the reduction in the total motor number N on the cargo. In the dynein Loa study we achieved quantitative agreement between theory and experiment, but here, for bidirectional transport, we were unable to do so. Thus, we conclude that although tugs-of-war likely exist some of the time, using this mechanism alone one cannot explain bidirectional motion—there must be an additional mechanism (likely enzymatic) that contributes to regulation of the motors.

One could wonder about whether we failed to find the right choice of parameters, but specific qualitative discrepancies between the theoretical predictions and experimental observations (discussed below) suggest to us that this is unlikely.

The Importance of Pauses. In a tug-of-war model, pauses occur when the opposite motors "battle," and as such are a crucial readout, sensitive to the tug-of-war process. The frequency of pauses is determined by a combination of the number of motors present on the cargos, and the on rates of those motors. The pause durations are determined both by the number of motors engaged in the tug-of-war, the individual motors' on rates, and the detachment kinetics of the motors under load. One key feature of tug-of-war models is that the more motors are present, the more opportunities for battles one has, and thus the higher the frequency of pauses. This was true for almost all variants of the tug-

of-war models we examined, but not observed experimentally. The only exception to this occurs when the motors detach easily (some exponential-detachment models), so that the majority of pauses are so short that they are undetected. In this case, pause frequency may be less affected by the number of motors present, but pause duration will be extremely short. A second qualitative feature of pauses/tug-of-war models is that more motors frequently lead to longer pauses; this can be seen experimentally in vitro in the detachment studies (Fig. 2). However, this change in pause duration is also not experimentally observed in the lipid-droplet system when the number of motors is altered.

The Relationship Between Run Lengths and the Number of Motors Present. For unregulated unidirectional motors, more motors move further (6, 12). If detachment kinetics of the motors are sufficiently fast above stall (e.g., in some variants of the exponential detachment models), this is also true for bidirectional models, because, e.g., one dynein motor stochastically attaching to oppose three kinesin motors is quickly overwhelmed and releases before there is a significant chance for additional dynein motors to bind and help it sustain the competition. However, for actual single-motor detachment kinetics (measured in vitro), the motors' off rates under load are slow enough that when a single motor stochastically attaches to oppose a group of opposite-polarity motors moving the cargo, it is able to "hold on" for a time comparable (or longer than) the typical on time of its compatriots. In this case, a stochastic attachment event from a single motor has a high probability of turning into a full-out tug-of-war between approximately evenly matched sets of opposite motors, and thus can cause a reversal. Then, for otherwise fixed parameters, the more motors present, the more tugs-of-war, and the shorter the travel of the cargo between pauses or reversals.

Qualitative Mismatch Between Theory and Experiments. Overall, as discussed above, in tug-of-war scenarios, for fixed parameter values, more motors lead to more frequent tugs-of-war, as long as a single motor can successfully (at least temporarily) pause a group of opposite-polarity motors. This occurs when the motors' detachment kinetics are not exponential above stall. Hence, in the models, more motors imply more pauses. Further, in the models, and confirmed in vitro, more motors tend to lead to longer pauses. We tested both these general properties in vivo, by comparing motion in wild-type embryos to motion in embryos with reduced kinesin on the LDs [reduced LD kinesin reduces number of engaged motors (14)]. Our analysis of motion in these two backgrounds shows that reduced motors did not lead to a decrease in pause frequency, nor a change in pause duration. Thus, in addition to quantitatively not matching the experimental data, the general trend predicted by the tug-of-war models is not observed in our experiments.

In any theoretical investigation, one makes simplifications. If a theory fails, one might question the simplifications, or whether the wrong parameter set was chosen, rather than concluding the theory is fundamentally wrong. Here, we ignore potential effects of NudE/Lis1 to decrease dynein's detachment under load (9). Whether this specific effect on dynein's motor output contributes to bidirectional transport is unclear, but if so, the effect would be to make the models even worse: Tugs-of-war would be more severe, and pauses would be even longer. In the most likely variants of the models, motion is already predicted to spend too much time paused.

The mean-field models have other difficulties. The stochastic models are better in vitro; the justification for ignoring this, and believing that the mean-field models will suddenly do better in vivo, is unclear. Further, our experiments clearly constrain the number of motors per wild-type droplet to between $N = 2.5$ and $N = 5$, and over this range pausing predictions are dramatically wrong: With real detachment kinetics, cargos spend twice as much time paused as they ought to, and for exponential detachment kinetics, they spend only half as much time paused.

Conclusion

As studied, neither the stochastic nor mean-field tug-of-war models describe our observations, and the difference in qualitative trends (see above) support the notion that slightly different choices of parameter values is unlikely to be better. Conceivably, there could be unknown/unconsidered factors that exist in vivo that very significantly modulate the properties of the motors (and the outcomes of tugs-of-war) in ways that we have not considered. Thus, although we favor the hypothesis that a significant portion of lipid-droplet directional switching does not result from unregulated tugs-of-war, this hypothesis should be revisited as new motor regulators are discovered.

In addition to providing strong indication that the tug-of-war picture is insufficient to capture all aspects of transport dynamics in vivo, our work provides a convenient template for future evaluations of the correspondence between tug-of-war models and experimental observations. Further studies across different motor species and in different in vivo environments should allow increasingly better understanding of the limits of tug-of-war models.

Methods

Quantitation of lipid-droplet motion was as described in ref. 14, and optical-trapping assays, data recording, particle tracking, and stalling-force analysis were performed as described in refs. 6 and 12. Theoretical modeling was done as described in ref. 8, with modifications described above. Further methods details are in the *SI Text*.

ACKNOWLEDGMENTS. We gratefully acknowledge dynein from Dr. Richard Vallee (Columbia University, New York, NY). Work done at the University of California, Irvine, was supported by National Institutes of Health/National Institute of General Medical Sciences Grant GM064624 to S.P.G. and GM079156 to C.C.Y. and S.P.G. Work done at the University of California; Davis, was supported by National Institutes of Health/National Institute of General Medical Sciences Grant GM068952 to A.M.

1. Gross SP (2004) Hither and yon: A review of bi-directional microtubule-based transport. *Phys Biol* 1:R1–R11.
2. Muller MJ, Klumpp S, Lipowsky R (2008) Tug-of-war as a cooperative mechanism for bidirectional cargo transport by molecular motors. *Proc Natl Acad Sci USA* 105:4609–4614.
3. Soppina V, Rai AK, Ramaiya AJ, Barak P, Mallik R (2009) Tug-of-war between dissimilar teams of microtubule motors regulates transport and fission of endosomes. *Proc Natl Acad Sci USA* 106:19381–19386.
4. Hendricks AG, et al. (2010) Motor coordination via a tug-of-war mechanism drives bidirectional vesicle transport. *Curr Biol* 20:697–702.
5. Gross SP, et al. (2000) Dynein-mediated cargo transport *in vivo*. A switch controls travel distance. *J Cell Biol* 148:945–956.
6. Vershinin M, Carter BC, Razafsky DS, King SJ, Gross SP (2007) Multiple-motor based transport and its regulation by Tau. *Proc Natl Acad Sci USA* 104:87–92.
7. Klumpp S, Lipowsky R (2005) Cooperative cargo transport by several molecular motors. *Proc Natl Acad Sci USA* 102:17284–17289.
8. Kunwar A, Vershinin M, Xu J, Gross SP (2008) Stepping, strain gating, and an unexpected force-velocity curve for multiple-motor-based transport. *Curr Biol* 18:1173–1183.
9. McKenney RJ, Vershinin M, Kunwar A, Vallee RB, Gross SP (2010) LIS1 and NudE induce a persistent dynein force-producing state. *Cell* 141:304–314.
10. Coppin CM, et al. (1997) The load dependence of kinesin's mechanical cycle. *Proc Natl Acad Sci USA* 94:8539–8544.
11. Carter NJ, Cross RA (2005) Mechanics of the kinesin step. *Nature* 435:308–312.
12. Mallik R, Petrov D, Lex SA, King SJ, Gross SP (2005) Building complexity: An in vitro study of cytoplasmic dynein with in vivo implications. *Curr Biol* 15:2075–2085.
13. Ori-McKenney KM, et al. (2010) A cytoplasmic dynein tail mutation impairs motor processivity. *Nat Cell Biol* 12:1228–1234.
14. Shubeita GT, et al. (2008) Consequences of motor copy number on the intracellular transport of kinesin-1-driven lipid droplets. *Cell* 135:1098–1107.
15. Petrov DY, et al. (2007) Studying molecular motor-based cargo transport: What is real and what is noise? *Biophys J* 92:2953–2963.
16. Gross SP, et al. (2002) Interactions and regulation of molecular motors in Xenopus melanophores. *J Cell Biol* 156:855–865.
17. Ally S, Larson AG, Barlan K, Rice SE, Gelfand VI (2009) Opposite-polarity motors activate one another to trigger cargo transport in live cells. *J Cell Biol* 187:1071–1082.
18. Ligon LA, Holzbaur EL (2007) Microtubules tethered at epithelial cell junctions by dynein facilitate efficient junction assembly. *Traffic* 8:808–819.